Construction and Building Materials 167 (2018) 1–14

Contents lists available at ScienceDirect

Construction and Building Materials

journal homepage: www.elsevier.com/locate/conbuildmat

Self-healing of concrete cracks by use of bacteria-containing low alkali cementitious material

Jing Xu *, Xianzhi Wang

Key Laboratory of Advanced Civil Engineering Materials (Tongji University), Ministry of Education, Shanghai 201804, China

HIGHLIGHTS

- A new type of carrier based on the low alkali cementitious material was developed.
- The carrier was very effective in preserving the bacterial activity.
- Cracks up to 417 μm was healed completely in 28 days by loading bacteria in the carrier.

ARTICLE INFO

Article history:
Received 9 October 2017
Received in revised form 31 January 2018
Accepted 4 February 2018

Keywords:
Concrete
Cracks
Self-healing
Bacteria
Carrier

ABSTRACT

Self-healing based on microbially-induced calcium carbonate precipitation has been proposed as a smart and environmentally friendly strategy for the repair of concrete cracks. It is advisable to incorporate bacteria-based healing agents in fresh state concrete during mixing. Although the selected bacteria are alkaliphilic spore-forming strains, they are still vulnerable to the harsh environment of concrete. In this paper, we developed a protective carrier for the bacteria by using calcium sulphoaluminate cement, which is a type of low alkali, fast hardening cementitious material. By regulating the composition of the carrier material and the content of healing agents, the compatibility of the carrier with both the healing agents and the concrete matrix was optimized. The carrier, which acted as a support for the bacteria, was effective in preserving the bacterial activity over a long period of time. After embedding this bacteria-based self-healing system in concrete, cracks up to 417 μm with a crack closure near 100% was achieved in 28 days. Compared with plain mortar, the regain ratios of the compressive strength and water tightness increased 130% and 50%, respectively. The research suggests the potential application of this novel microbial self-healing system in extending the life span of concrete.

1. Introduction

Since the crystal formation by bacteria as a general phenomenon was revealed almost half a century ago, it has been applied in a variety of fields such as geological engineering, oil industry, historic preservation, and civil engineering [1,2]. A series of applications involve plugging of rock system for oil recovery enhancement, consolidating and strengthening of sand columns, and protection of ornamental stones were achieved by bio-deposition or bio-cementation [3–10]. In most cases, calcinogenic bacteria were used that calcium carbonate ($CaCO_3$) was produced during the process, which is known as microbially induced carbonate precipitation (MICP) [11–13]. Recently, this technique has been explored for the crack remediation and durability improvement of concrete [14–18].

For concrete, a most used building material worldwide, cracking is almost unavoidable due to its inherent brittleness and the complex service environments. Although the presence of cracks may not impair the strength and integrity of the concrete structure immediately, it will reduce the durability of concrete because aggressive species like chlorides and sulfates can penetrate into the matrix through crack paths, particularly when a continuous network is formed by micro-cracks. Thus, timely repair work is needed. General repair methods often require periodical inspection and maintenance, which are quite laborsome and expensive. Besides, repair agents are applied from outside that deep micro-cracks may not be possible to be healed due to the limit of penetration. In order to solve these problems, an alternative method based on self-healing process was proposed [19].

* Corresponding author.
E-mail address: 0610060014@tongji.edu.cn (J. Xu).

https://doi.org/10.1016/j.conbuildmat.2018.02.020
0950-0618/

As a matter of fact, concrete is capable of sealing micro-cracks in certain conditions, and it is known as "autogenous healing". This phenomenon is primarily attributed to hydration of unhydrated cement particles or chemical precipitation of $CaCO_3$. Another category of self-healing is so-called "autonomous healing". By simply adding specific healing agents in fresh state mixture, cracks will be healed from inside to outside in hardened concrete via the release of healing agents [20,21]. However, most studied healing agents are chemically based. Under such circumstances, self-healing of concrete by MICP was considered in the past decades. Compared with other types of healing agents, bacterially mediated $CaCO_3$ is compatible with concrete and environmentally friendly. Up to now, three bacterial metabolic pathways associated with $CaCO_3$ precipitation have been investigated for concrete crack self-healing. The first pathway is the enzymatic hydrolysis of urea, which is carried out by ureolytic bacteria [22–25]. The second one is the oxidation of organic carbon [26–30]. Another pathway is related to the denitrification process under anoxic conditions [31,32]. Among all the pathways of the precipitated bio-$CaCO_3$, ureolysis-based type is easier to operate and control. It is also known for its high efficiency that the reaction rate of biogenic urea hydrolysis is approximately 10^{14} times faster than the chemical rate [21].

Because of the alkalinity nature of concrete, alkaliphilic spore forming strains were used for self-healing. Bacterial spores, which are dormant state of cells, can withstand heat, dry, various chemicals, and have much longer shelf life. The prerequisite of self-healing is that spores together with relevant nutrients must be incorporated during casting. However, directly adding bacteria in matrix is inadvisable due to the harsh environment inside concrete. Jonkers et al. [27] reported that bacterial activity decreased significantly in the high pH (>12) environment and bacterial cells (1–3 μm) could be squeezed or crushed owing to the decrease of pore size (<0.5 μm) along with the hydration process of concrete. Therefore, encapsulation or immobilization of bacteria in a protective carrier is preferable. A variety of carriers have been studied previously. Jonkers et al. [33–35] proposed a self-healing system by loading bacterial spores and other bio-reagents in expanded clay particles. The maximum crack width that can be healed reached 0.46 mm after 100 days of incubation, compared with only 0.18 mm for the control. De Belie et al. [36–40] tested a series of carriers including hollow glass fibers, microcapsules, diatomaceous earth, silica gel, polyurethane, hydrogel, and granular activated carbon. Superiority of self-healing appears after several weeks incubation of directly immersion or wet-dry cycle curing. Compared with the reference specimens, the strength regain increased 60% while the water permeability decreased about 1–2 orders of magnitude. In our previous research, air voids were introduced by air entraining agents to accommodate bacteria [41]. The recovery of strength and modulus after bacterially-mediated healing was almost two times higher than that of control. Above all, a preferable protective carrier not only provide a shelter for bacteria, but has limited negative effects on bacterial activity and cement hydration.

In the present study, we tried to develop a bacterial healing system by encapsulating healing agents in calcium sulphoaluminate cement, a type of low alkali cementitious material. It is a fast setting and hardening binder that often used for concrete repair. In this manner, the low alkali binder serves as a protective carrier which is compatible with concrete and not detrimental to the viability of bacteria. The aim of this study is to quantify the self-healing ability of concrete based on this system.

2. Materials and methods

2.1. Cultivation of bacteria

A ureolytic type bacterium, *Sporosarcina pasteurii* ATCC 11859, was purchased from the China General Microbiological Culture Collection Center (CGMCC). Bacterial strains were cultured in liquid medium according to the supplier's recommendation and supplemented with manganese to enhance spore formation. The medium contained 5 g peptone, 3 g beef extract, 20 g urea, and 0.01 g $MnSO_4{\cdot}H_2O$ per liter of distilled water. Urea was separately sterilized by filtration through a sterile 0.2 μm filter and mixed with other ingredients which were autoclaved at 121 °C for 20 min. The pH was adjusted to 8 ~ 8.5 by using filter sterilized NaOH or HCl solution. Cultures were aerobically incubated at 20 °C on a water-bath shaker operated at 100 rpm. Growth was regularly checked quantitatively by an optical microscopy. The incubation was performed for over 14 days until more than 90% of cells were spores. The cells were harvested by centrifuging the culture (4000 rpm, 20 °C) for 10 min and resuspension in sterile saline solution (0.15 M NaCl), then subjected to a pasteurization process of 20 min in a 80 °C water bath in order to eliminate vegetative cells. The suspension of spores (about 10^9 spores/mL) was stored in a 4 °C fridge for future use.

2.2. Tests on encapsulation material

The calcium sulphoaluminate cement (42.5R, Qilin Co. Ltd, China) was used as the encapsulation material for bacterial spore loading owing to its nature of low alkalinity. Silica fume (Elkem Materials) was added in the amount of 0%, 20%, and 40% by mass of calcium sulphoaluminate cement to further reduce the alkalinity of the material. Table 1 shows the chemical composition of the cementitious materials. In order to evaluate the alkalinity of the encapsulation material, a binder solution was made by a large water-to-binder ratio (w/b) of 10 to ensure a thorough hydration. The calcium sulphoaluminate cement together with different amount of silica fume were mixed with water in a 100 mL falcon tube and put on a shaker at 100 rpm for 1 h. Then the mixture was filtered and the pH of the filtrate was measured by a pH probe (Mettler Toledo pH Meter Kit). For comparison, Ordinary Portland cement (P·O 42.5, Conch Co. Ltd, China) whose composition is shown in Table 1 was tested by the same procedure. Three replicates were tested in each series.

Nutrients include peptone and beef extract should also be loaded in the encapsulation material. The influence of the nutrients and bacterial spores on the hydration of calcium sulphoaluminate cement was investigated. At a certain spore addition (1mL suspension of spores with concentration of 10^9 cells/mL), varied concentration of nutrients (0%, 1%, 1.5%, 2%, 3%, 4% in mass of calcium sulphoaluminate cement) were used. Table 2 shows the detailed

Table 1
Chemical composition of the used cementitious materials.

Materials	CaO	SiO_2	Al_2O_3	Fe_2O_3	SO_3	MgO	K_2O	TiO_2	P_2O_5
Ordinary Portland cement	54.86	21.86	6.33	2.61	2.66	2.60	0.68	0.27	\
Calcium sulphoaluminate cement	43.00	8.28	33.36	1.95	7.90	1.69	0.23	1.35	0.14
Silica fume	0.29	93.80	0.26	\	0.45	0.56	0.54	\	\

Table 2
Arrangement for the investigation of the effects of spores and nutrients on the calcium sulphoaluminate cement.

Series	Calcium sulphoaluminate cement (g)	Water (g)	Suspension of spores (mL)	Peptone (g)	Beef extract (g)
R	100	49	\	\	\
S	100	49	1	\	\
SN1	100	49	1	0.62	0.38
SN1.5	100	49	1	0.94	0.56
SN2	100	49	1	1.25	0.75
SN3	100	49	1	1.88	1.12
SN4	100	49	1	2.50	1.50

experimental arrangement. The initial and final setting time of the mixture were tested according to ASTM C191-04b [42].There were three replicates in each series.

2.3. Activity of encapsulated spores

2.3.1. Encapsulation procedure

10 g calcium sulphoaluminate cement and 2 g silica fume were first mixed with 5 g water, and then 1 mL bacterial spore suspension (10^9 cells/mL) was added. The mixture was mixed at 200 rpm for 5 min by a rotary mixer. After casting in cubic molds of 20 mm × 20 mm × 20 mm dimension, the samples were demolded after 2 h and then cured in a standard curing room (20 ± 2 °C, 100% RH) for 3 days. The hardened cubes were crushed, oven-dried at 40 °C, and ground until all the powder particles can pass through an 80 μm sieve.

The morphology of the powder particles was observed by scanning electron microscope (SEM) under a low vacuum mode. A scanning electron microscopy (Hitachi S-3400) was used. The pore properties of the particles were probed by low-field nuclear magnetic resonance (LF-NMR) relaxometry. About 1 g of sample was pre-saturated with water before being gently packed into a cylinder glass tube and sealed for NMR test. A low frequency (^{1}H resonant frequency of 12 MHz) NMR spectrometer (NMRC12-010 V-T, Niumag Corp., China) was used with a permanent magnetic field of 0.28 T. The spin–spin relaxation time (T_2) was determined by using a Carr–Purcell–Meiboom–Gill (CPMG) pulse sequence. After the initial exciting π/2 rf pulse, 1500 spin echoes were generated by successive π rf pulses. The π/2 rf pulse and the π rf pulse were set to 4.6 μs and 9.2 μs, respectively. The inter echo time was set to τ = 40 μs. Each CPMG signal was averaged over 32 scans to obtain a good signal-to-noise ratio (S/N). The interval between each repetition was 100 μs. All relaxation time measurements were performed at 32 °C. Assuming that the total magnetization decay is given by a superposition of exponential decays, the distributions of T_2 were calculated by a regularized inverse Laplace transformation by using InvFit software attached to the instrument. The T_2 relaxation times can be interpreted in terms of the pore radius R of the material assuming that the pores are in cylindrical shape [43]

$$\frac{1}{T_2} = \frac{\lambda}{T_{2s}} \cdot \frac{S}{V} \approx \frac{\lambda}{T_{2s}} \cdot \frac{2}{R} \tag{1}$$

where λ is the thickness of one single layer of water and is 0.3 nm, T_{2s} is the surface relaxation time which can be assumed to be 60 μs in this system [44], S and V are the total surface area and volume of the pore. For the material with a continuous pore distribution, the measured echo intensity M at time t can be written as

$$M(\mathrm{t}) = M_0 \int P(T_2) \exp\left(-\frac{t}{T_2}\right) dT_2 \tag{2}$$

where $P(T_2)$ is the distribution function of T_2. Substituting Eq. (1) into Eq. (2) yields

$$M(\mathrm{t}) = M_0 \int P'(R) \exp\left(-\frac{2\lambda}{T_{2s}} \cdot \frac{t}{R}\right) dR \tag{3}$$

Therefore, the distribution of pore radius R can be deduced from the distribution of relaxation time T_2, while the intensity of the signal of T_{2i} is equivalent to the volume of pores with corresponding pore radius R_i. After testing, the particles were weighed and then put into 105 °C oven for drying until the weight kept constant. The mass difference before and after drying was assumed to be the total volume of pores.

2.3.2. Treatment by simulated concrete pore solution

In order to simulate the high pH environment inside concrete, a concrete pore solution was prepared by Ordinary Portland cement and water with water-to-cement (w/c) ratio of 10. The preparation procedure which consists of mixing, shaking, and filtering was the same as described in Section 2.2. For the treatment on spores without encapsulation, 1 mL spore suspension (10^9 cells/mL) was mixed with 10 mL concrete pore solution and left to rest for 24 h. After that, spores were collected by repeated centrifugation and washing by sterile distilled water. For the treatment on encapsulated spores, 18g dry bio-powder was put in a filtering tea bag, which was then submerged in 100 mL concrete pore solution for 24 h. After that, the tea bag was taken out and rinsed repeatedly by sterile distilled water. Then the tea bag was oven-dried at 40 °C until the mass kept constant. Dry powders were collected from the opened tea bag.

2.3.3. Evaluation of bacterial activity

The amount of urea decomposed by spores was used as an index to evaluate the activity of the spores with or without encapsulation. Urea concentration measurement was based on a colorimetric method as described by Douglas and Bremner [45]. A visible spectrophotometer V-1200 was used for the colorimetric tests. 1 mL spore suspension or 18 g dry bio-powder with and without treatment, respectively was added to 100 mL growth medium, which consists 5 g peptone, 3 g beef extract, and 20 g urea per liter of distilled water. As a control, an equivalent amount of abiotic dry powders were added to the same medium. The amount of urea decomposed during 10 days was measured by the colorimetric method. In the meantime, the bacterial cell density was measured by the plate-counting method. Tests were performed at 20 ± 2 °C. Three replicates were used in each series.

2.4. Preparation of mortar specimens

Mortar specimens was made by Ordinary Portland cement, local natural sand with a specific gravity of 2.65g/cm^3, and tap water. The w/c was 0.5 and sand-to-cement ratio (s/c) was 3. The mix proportions of the specimens are shown in Table 3. Reference specimens are the mortars without any addition. Abiotic control specimens are the ones with encapsulated dry powder added, including only nutrients (beef extract and peptone). Microbial specimens are the ones with encapsulated dry powder added,

Table 3
Mix proportions of the tested mortar specimens.

Series	Cement (g)	Water (g)	Sand (g)	Encapsulated dry powder (g)	Calcium nitrate (g)	Urea (g)	Basalt fiber (g)	Water reducing agent (g)
Reference	250	125	750	\	\	\	8.3	0.8
Abiotic control	250	125	750	12.5[a]	1.5	2.5	8.3	1.0
Microbial	250	125	750	12.5[b]	1.5	2.5	8.3	1.0

[a] One gram of dry powder was loaded with 5.5 mg peptone and 3.3 mg beef extract.
[b] One gram of dry powder was loaded with 5.5 mg peptone, 3.3 mg beef extract, and 10^7 cells of spores.

including both nutrients and bacterial spores. Basalt fibers were added to facilitate the formation of cracks while keeping the integrity of the specimens. A water reducing agent based on polycarboxylic acid type F was used to adjust the fluidity of the mixtures. Urea and calcium nitrate were added directly into the matrix.

During the process of mixing, a rotary mixer with a flat beater was used. Fibers were added in water and then the water reducing agent was added and mixed for about 1 min. Then the encapsulated dry powder, urea, and calcium nitrate, if any, together with cement and sand were mixed in the mixer for 3 min. After pouring into cubic molds of 50 mm × 50 mm × 50 mm dimension, an external vibrator was used to facilitate compaction and decrease the amount of air bubbles. The specimens were demolded after 24 h and then cured in a standard curing room (20 ± 2 °C, 100% RH) for 27 days. Five specimens were prepared for each series.

2.5. Cracks creation and self-healing incubation

Mortar cubes were subjected to a compressive stress at a loading speed of 0.01 mm/s under a displacement control mode. Before the test, all specimens were oven-dried at 40 °C until the weight varies within 0.1%. The compressive loading test was carried out on a SANS Universal Testing Machine. After peak loading, the final displacement was controlled as the load stopped by that one single crack appears at any side of the surface. The compressive strength was recorded by the peak load. The initial crack width was in the range of 20–450 μm, and the initial crack area for each cube was estimated as in the range of 5–15 mm^2.

Following the cracking, specimens were subjected to wet-dry cycles for 4 weeks. During one wet-dry cycle, the specimens were submerged in water for 1 h and exposed to air (60 ± 10% RH) for 11 h. The incubations were performed at 20 ± 2 °C.

2.6. Evaluation of self-healing efficiency

2.6.1. Visual inspection

Before and after the wet-dry cycles of incubation, surface of the specimens was checked by optical microscopic inspection. Self-healing of cracks were quantitatively analyzed by an image processing software "Image-Pro plus". Specimens were exposed to ambient air condition (20 ± 2 °C, 60 ± 10% RH) during inspection. The crack closure was evaluated at the end of 28 days of treatment. Crack healing ratio was calculated by the equation

$$\text{Crack healing}\,\% = \frac{CW_0 - CW_{28}}{CW_0} \times 100 \quad (4)$$

where CW_0 and CW_{28} are the initial crack width and the crack width measured at 28 days, respectively (μm). The percentage of the crack closure was obtained by the equation

$$\text{Crack closure}\,\% = \frac{CA_0 - CA_{28}}{CA_0} \times 100 \quad (5)$$

where CA_0 and CA_{28} are the total area of the initial cracks and the cracks measured at 28 days, respectively (μm).

2.6.2. Capillary water absorption

Capillary suction tests were performed to quantitatively assess the water tightness of the specimens before cracking, after cracking, and after healing. The specimens were first oven-dried at 40 °C until the mass change in 24 h was less than 0.1%, and then fully submerged in tap water with the water level 5 cm higher than the top surfaces. The mass change of the specimens was recorded at regular time intervals. A wet towel was used to remove the remaining water droplets on the surface before weighing. Tests were done in an atmosphere of 20 ± 2 °C and 60 ± 10% RH. By depicting the relation between the amount of water absorbed and time, the sorptivity coefficient S can be calculated by a power function as follow,

$$\frac{Q}{A} = S \cdot \sqrt{t} \quad (6)$$

where Q is the amount of water absorbed (g), A is the cross section of the specimen in contact with water (cm^2), t is the time (min), and S is the sorptivity coefficient (g cm^{-2} $min^{-1/2}$). Then the regain ratio of the water tightness r_S can be calculated by

$$r_s\% = \frac{S_{bc} - S_{ac}}{S_{bc} - S_{ah}} \times 100 \quad (7)$$

where S_{bc}, S_{ac}, and S_{ah} are the sorptivity coefficient before cracking, after cracking, and after healing, respectively.

2.6.3. Mechanical properties

After 28 days incubation, specimens were again oven-dried as described in Section 2.5, and then subjected to compressive tests until complete damage by using the same mechanical testing system. The compressive strength after self-healing were recorded as corresponding to the peak load, and the strength regain ratio r_R was calculated by

$$r_R\% = \frac{R_{sh}}{R_f} \times 100 \quad (8)$$

where R_f is the compressive strength at first loading (MPa), R_{sh} is the compressive strength after self-healing (MPa).

2.6.4. Characterization of precipitates

Upon the complete damage by the mechanical tests, two pieces of fragments with an area of 4 mm^2 and thickness of 2 mm were cut from the crack mouth. Precipitates were scraped and collected from one piece for X-ray diffraction (XRD) analysis. Powder samples were scanned from 5° to 75° 2θ by an X-ray diffractometer (Rigaku D/MAX 2550VB3) with a Cu anode (40 kV and 100 mA). The precipitated surfaces of the second piece were coated by carbon (~20 nm thickness) for SEM analysis. A scanning electron microscopy (FEI Nova NanoSEM 450) coupled with energy dispersive X-ray spectroscopy (EDS) was used. Morphologies were obtained by secondary electron imaging (SEI).

3. Results

3.1. Encapsulation material

The alkalinity of the encapsulation material was evaluated by a binder solution with a large *w*/*b* ratio. The pH values of the solutions are shown in Fig. 1. For Ordinary Portland cement solution, pH of 12.8 was observed. In comparison, pH value of the calcium sulphoaluminate cement was 11 because of its low alkalinity nature. An addition of silica fume could reduce the pH value. However, further reduction of pH was insignificant when the addition of silica fume increased from 20% to 40%.

The influence of spores and nutrients (beef extract and peptone) on the setting time of the calcium sulphoaluminate cement is shown in Fig. 2. The addition of spores has negligible effect on the setting time. The increase of both initial and final setting time was insignificant until the addition of nutrients exceeded 1.5%; the setting time increased remarkably by the addition of nutrients higher than 3%.

3.2. Activity of spores after encapsulation and in simulated concrete pore solution

The bacterial ureolytic activity was assessed by the amount of urea degradation and cell growth (Fig. 3). Free spores showed the highest ureolytic activity that urea was almost depleted after about one day. The density of free cells increased by one order of magnitude during the first day. The proportion of decomposed urea was about 50% after 10 days for encapsulated spores, which indicates a loss of bacterial activity by encapsulation. The rapid growing phase was not evident until the fifth day for encapsulated spores. No obvious urea decomposition and cell growth occurred for abiotic powder series. After being treated by the high alkaline simulated concrete pore solution, the lag phase of cell growth seemed to be slightly prolonged and urea was completely decomposed after two days. This phenomenon is also applicable to the encapsulated spores treated by high pH solution. Wang et al. [39] had similar findings that the spores did not germinate until the high pH solution was removed. In contrast, the amount of urea decomposition by encapsulated spores after treatment was nearly the same as the one without treatment after 10 days.

Fig. 4 shows the SEM images of particles from hydrated calcium sulphoaluminate cement with 20% silica fume. Some hydration products in the form of needle or rod shaped crystals with size smaller than 2 μm were found for particles without loading

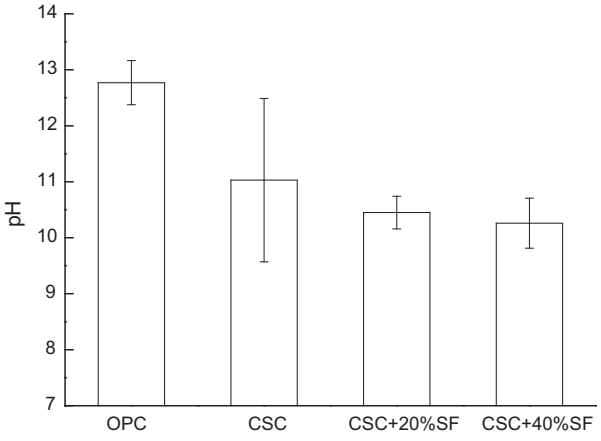

Fig. 1. pH values of the binder solution for different compositions of cementitious materials, OPC – Ordinary Portland cement; CSC – calcium sulphoaluminate cement; SF – silica fume.

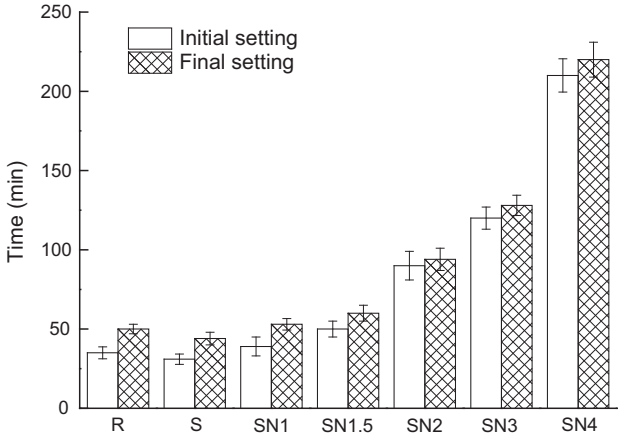

Fig. 2. The influence of spores and nutrients on the setting time of the calcium sulphoaluminate cement.

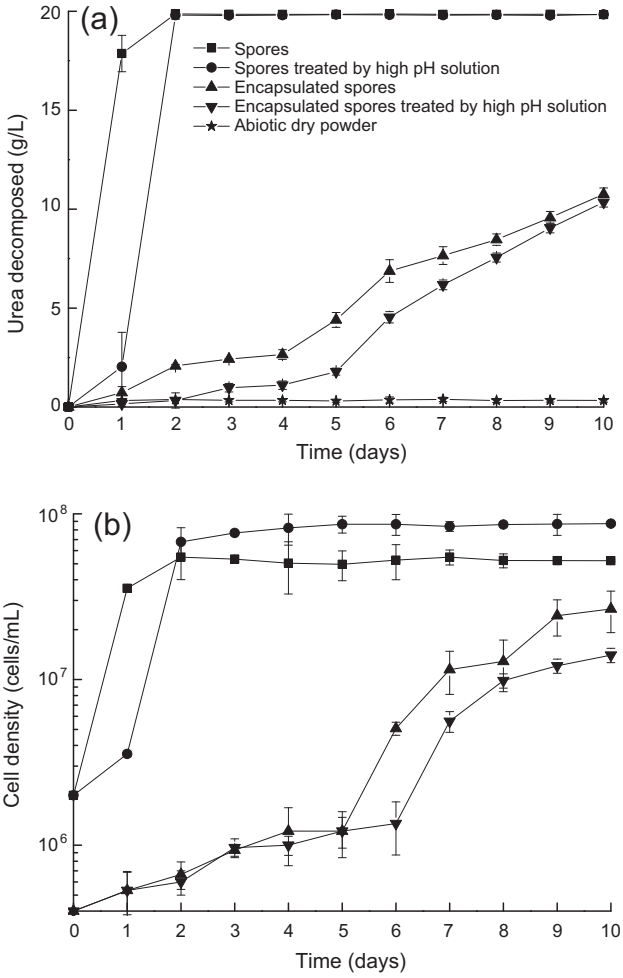

Fig. 3. Activity of free spores or encapsulated spores with and without treatment by simulated pore solution, (a) urea degradation; (b) cell density.

(Fig. 4a). These crystals were possibly related to ettringite. After encapsulation, bacterial cells with typical size around 1 μm could be identified in the structure (Fig. 4b). The pore size distribution of the particles is presented in Fig. 5. LF-NMR analysis revealed two major pore size classes, i.e. of 0.01–0.1 and 0.1–1 μm. The most probable pore size was around 0.4 μm. By the addition of

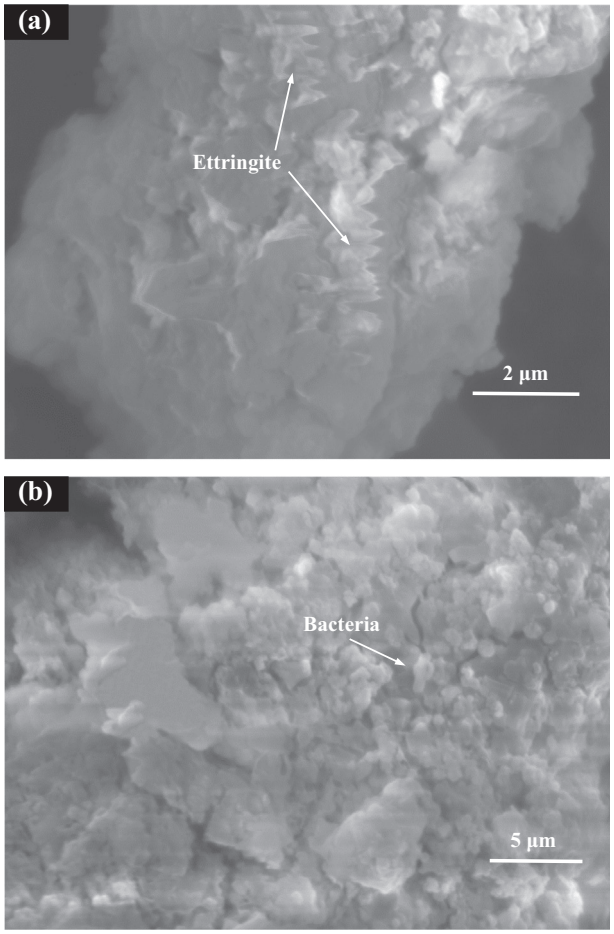

Fig. 4. SEM micrographs of carrier particles, (a) without encapsulation; (b) encapsulated with bacteria.

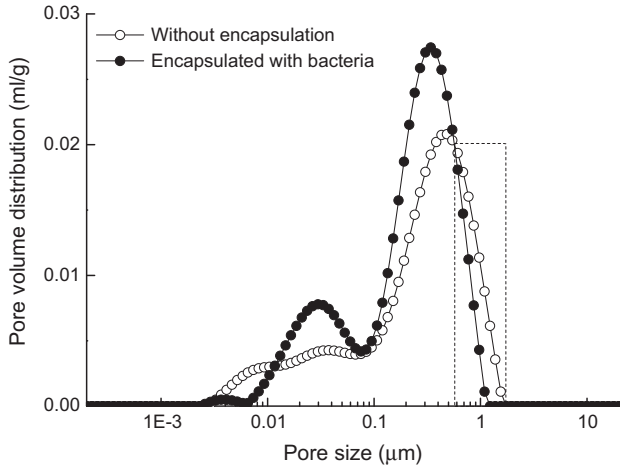

Fig. 5. Pore diameter size distribution of carrier particles with and without encapsulation.

spores, a slight shift from larger pores to smaller pores was observed in the pore size range of 0.6–1.6 μm (as indicated by the dashed box), which is exactly the typical size class of bacterial spores. The decreasing of pore size should be attributed to the filling by spores.

3.3. Visualization and quantification of crack healing

Before and after 28 days incubation, healing of cracks was visually inspected by an optical microscopy. Similar crack healing state appeared in the same series. Thus, one out of five specimens was selected in each series. As for the reference specimens, almost no precipitation occurred in the cracks after water curing (Fig. 6a). Small amount of precipitates were found in the cracks of specimens with the addition of nutrients after incubation (Fig. 6b). The appearance of the specimens with the addition of both spores and nutrients differed greatly. Not only the cracks were completely filled, but the surface of the specimens were partly covered by white precipitates after 28 days healing. Some pores were also filled by the deposits (Fig. 6c).

By using the image processing tool, the statistical analysis results are shown in Fig. 7 and Table 4. Reference specimens without any addition showed quite limited crack-healing potential that crack filling occurred in widths around 36 μm, and the maximum crack width could be healed was 56 μm. The abiotic control specimens, which refer to the ones containing encapsulation material loaded with only nutrients, showed better sealing performance than the plain mortar. The average and the maximum crack widths could be healed were 146 μm and 244 μm, respectively, while cracks up to 150 μm were closed completely. The addition of bacteria further enhanced the crack healing capability. Following 28 days incubation, crack healing for the widths up to 417 μm and complete crack healing up to 394 μm were achieved. The percentage of crack closure for the bacteria-based mortar specimens was almost 100%, which was twice of the abiotic control ones, and about 15 times of the reference specimens, respectively. Quantification of crack-healing verified the conclusion based on the visual inspection that crack-healing was profoundly improved by bacteria-mediated precipitation.

3.4. Capillary water absorption

After incubation, all the specimens showed a remarkable reduction of the amount of water absorption. However, the degree of reduction varied and the tendency was highly in line with the crack-healing condition (Fig. 8). Almost a full recovery of the water tightness was found for the microbial series after incubation that the amount of water absorption was very close to the amount before cracking. When comparing the sorptivity coefficient after healing, the trend was revealed as: Reference > Abiotic control > Microbial (Table 4). The microbial specimens showed the highest regain ratio of water tightness of about 95%, which is about 1.5 times of the reference ones.

3.5. Mechanical properties after healing

Table 4 shows the compressive strength of specimens before and after healing. At first loading, there was no significant difference among all the series, which indicates that the addition of encapsulation material in the form of hydrates of calcium sulphoaluminate cement would not have a negative effect on the mechanical properties of the matrix. After 28 days incubation, distinctive performances of the strength regain were noticed. The bacteria-based specimens achieved the highest regain ratio of strength, which is about 2.3 times of the reference ones. This is expected due to the nearly complete healing of cracks by bacterially-induced precipitation. The mechanical testing results were in good agreement of the visual inspection and water absorption measurements.

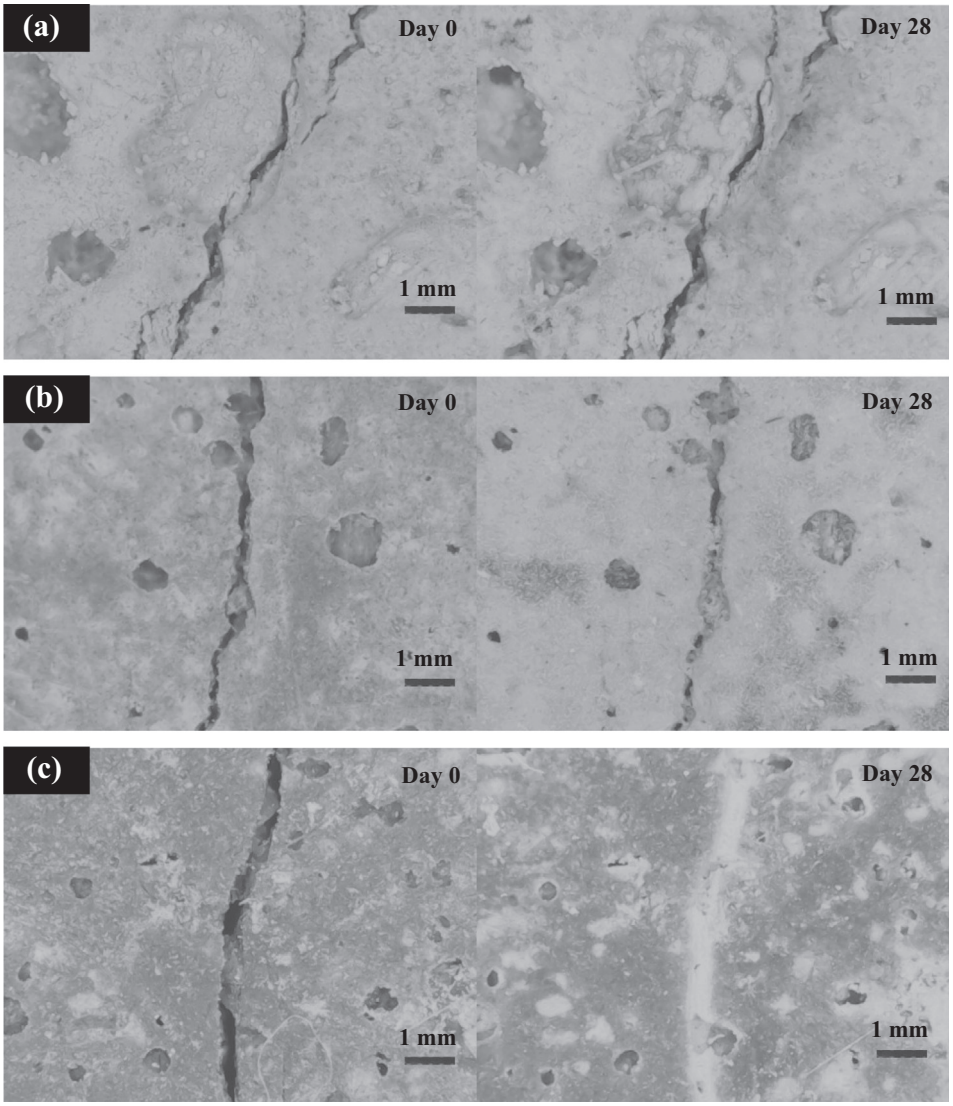

Fig. 6. Photomicrographs showing the healing of cracks before and after 28 days incubation, (a) reference; (b) abiotic control; (c) microbial.

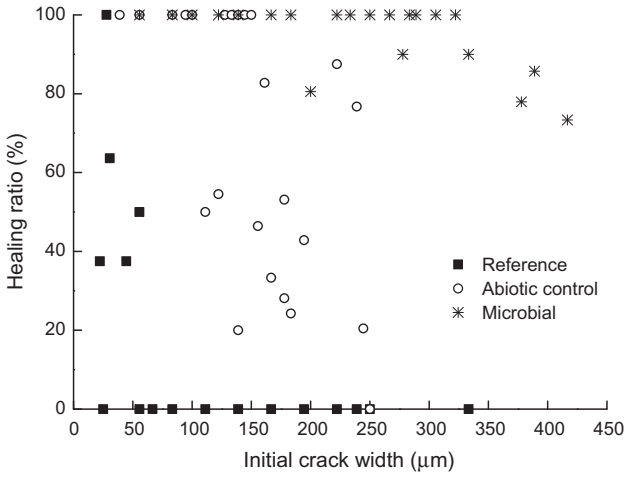

Fig. 7. Statistical analysis of the crack healing.

3.6. XRD/SEM analyses

Fig. 9 shows the XRD patterns of precipitates in all series. In addition to silica sand phase, hydration products such as portlandite and ettringite were found for reference mortar. Calcite appeared as one of the primary component for the other two series. Mostly C—S—H gel phase and portlandite minerals in plate shape were dominant inside the cracks of the reference mortar (Fig. 10a1 and a2). Formation of calcite appeared as small rhombohedral grains in size of ~ 2 μm was observed for abiotic control series (Fig. 10b1 and b2). Larger $CaCO_3$ crystals in the form of calcite were found on the crack walls of the bacteria containing specimens (Fig. 10c1). Compared to the abiotic control, calcite crystals seemed much more abundant in the microbial series. This could partly explain the higher healing efficiency obtained by the microbial specimens. Additionally, traces of bacteria could be clearly identified (Fig. 10c2). The information of chemical composition collected from EDS analyses verified the XRD results. Besides, the existence of N element confirmed the addition of organic matters in abiotic control and microbial specimens.

Table 4
Summary of the self-healing efficiency.

Series	Average width of healed cracks (μm)	Maximum width of healed cracks (μm)	Maximum width of 100% healed cracks (μm)	Percentage of crack closure (%)	S_{bc} ($g \cdot cm^{-2} \cdot min^{-1/2}$)	S_{ac} ($g \cdot cm^{-2} \cdot min^{-1/2}$)	S_{ah} ($g \cdot cm^{-2} \cdot min^{-1/2}$)	r_S (%)	R_f (MPa)	R_{sh} (MPa)	r_R (%)
Reference	36 ± 4	56 ± 4	28 ± 3	6.5 ± 2.2	0.004 ± 0.001	0.044 ± 0.001	0.019 ± 0.001	63 ± 4	45.4 ± 3.1	16.8 ± 3.3	37 ± 5
Abiotic control	146 ± 14	244 ± 16	150 ± 10	56.7 ± 11.3			0.010 ± 0.002	85 ± 6	46.5 ± 3.8	21.4 ± 3.4	46 ± 4
Microbial	219 ± 20	417 ± 15	394 ± 10	99.3 ± 0.3			0.006 ± 0.001	95 ± 4	46.8 ± 5.0	39.3 ± 6.1	84 ± 5

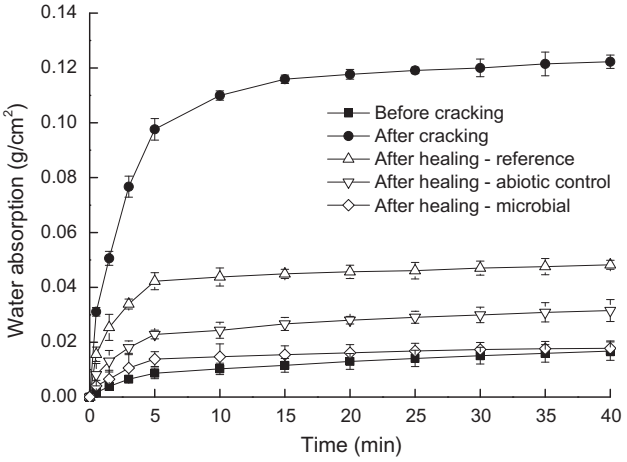

Fig. 8. Water absorption of specimens in each series as a function of time.

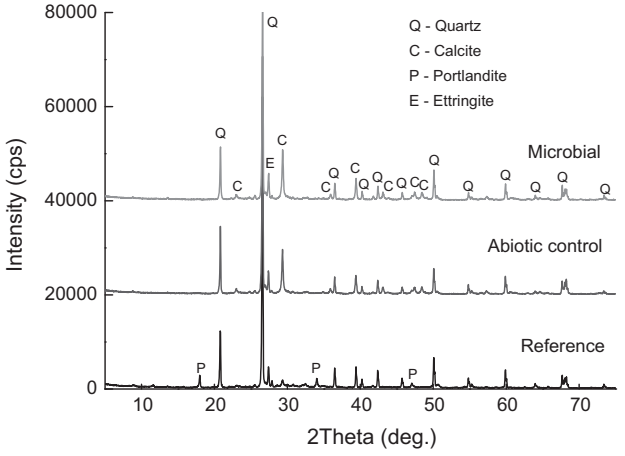

Fig. 9. XRD analysis of deposits collected from the crack mouth after 28 days incubation.

4. Discussion

4.1. Preparation of encapsulation material and built-in microbial self-healing system

In this work, we proposed a new type of encapsulation material by using calcium sulphoaluminate cement for the protection of bacteria. The microbial-based self-healing system was highly dependent on the selection and preparation of this encapsulation material, which include but are not limited to the considerations as follows.

4.1.1. Potential to provide protection for bacteria

As a protective carrier, it is of importance that it serves as a shelter for bacteria while keeping the bacteria as active as possible. As indicated by the amount of urea decomposition, the encapsulation of spores by calcium sulphoaluminate cement resulted in a loss of bacterial activity compared with free spores, possibly due to the damage of some cells during the encapsulation process. However, a rapid growth of cells and a speed-up of urea decomposition were observed after 5 days (Fig. 3), implying that the bacterial activity can be preserved by the carrier over a long period. A close inspection would be helpful for the explanation to this phenomenon. When spores were encapsulated, the powder particles seemed more porous than unloaded ones. The porous structure

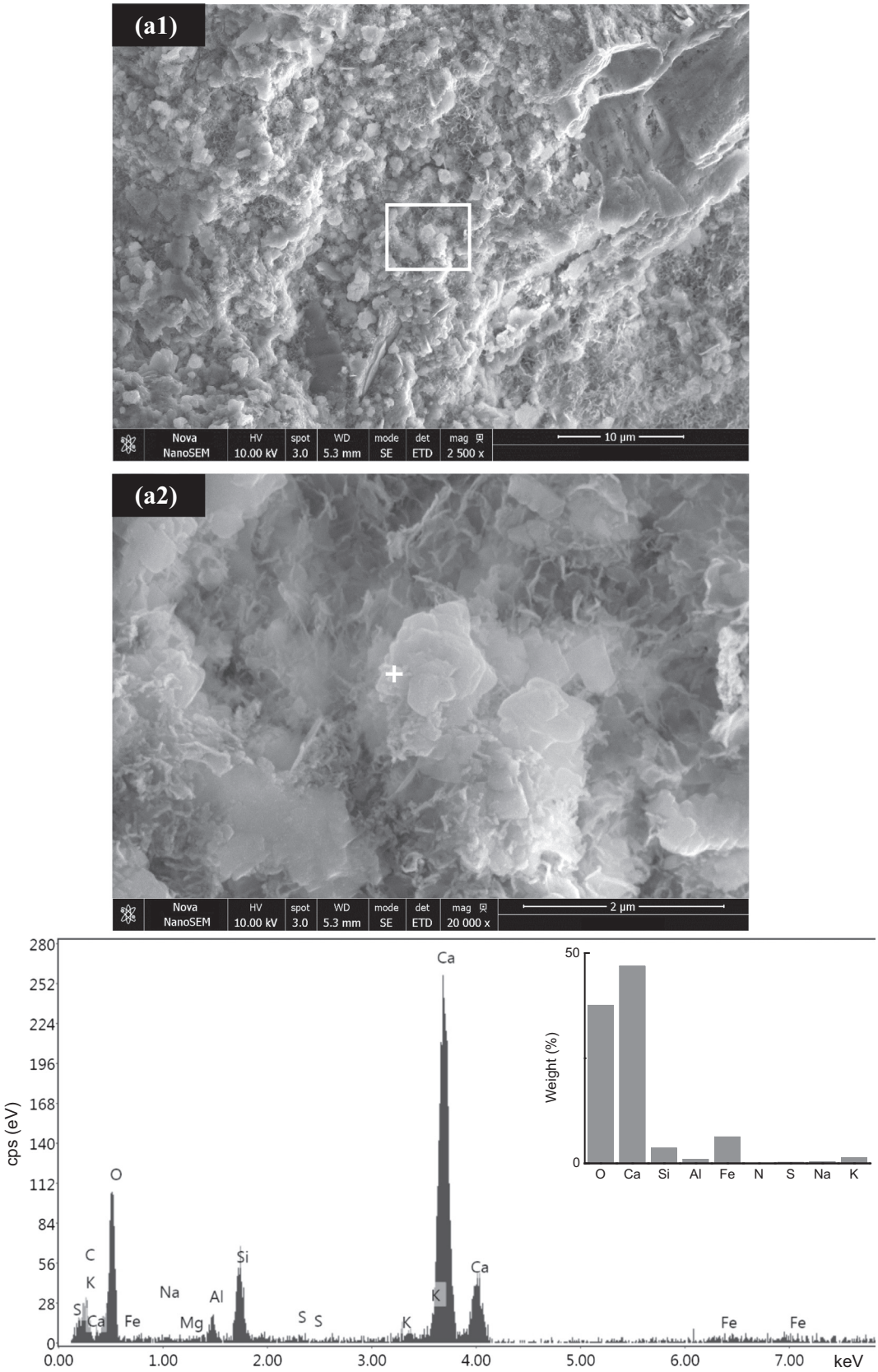

Fig. 10. SEM micrographs and EDS analyses of precipitates at the crack mouth after 28 days incubation, (a1) and (a2) reference; (b1) and (b2) abiotic control; (c1) and (c2) microbial, '□' shows the magnified area, '→' shows traces of bacteria, '+' shows the points analyzed via EDS.

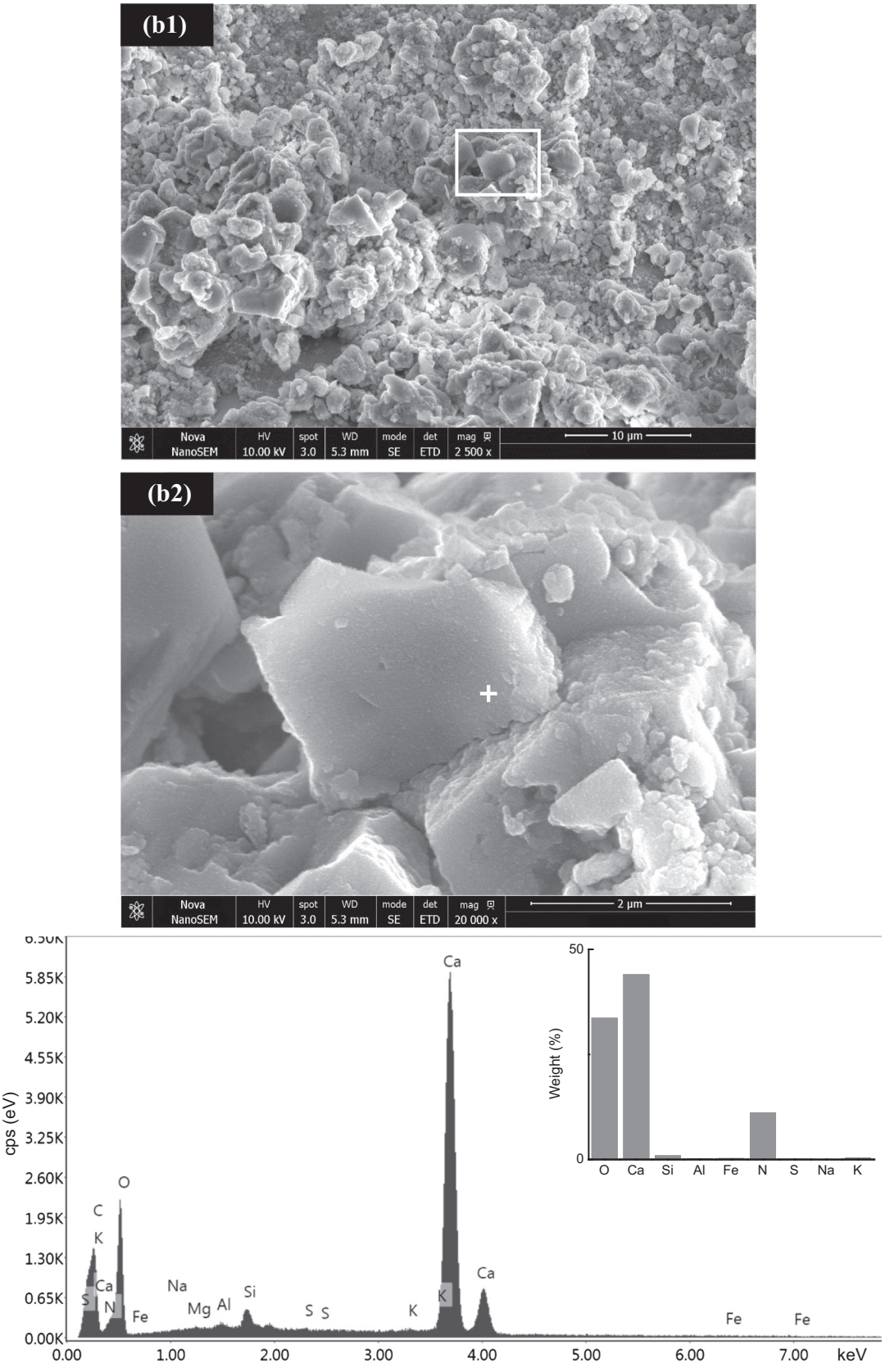

Fig. 10 (*continued*)

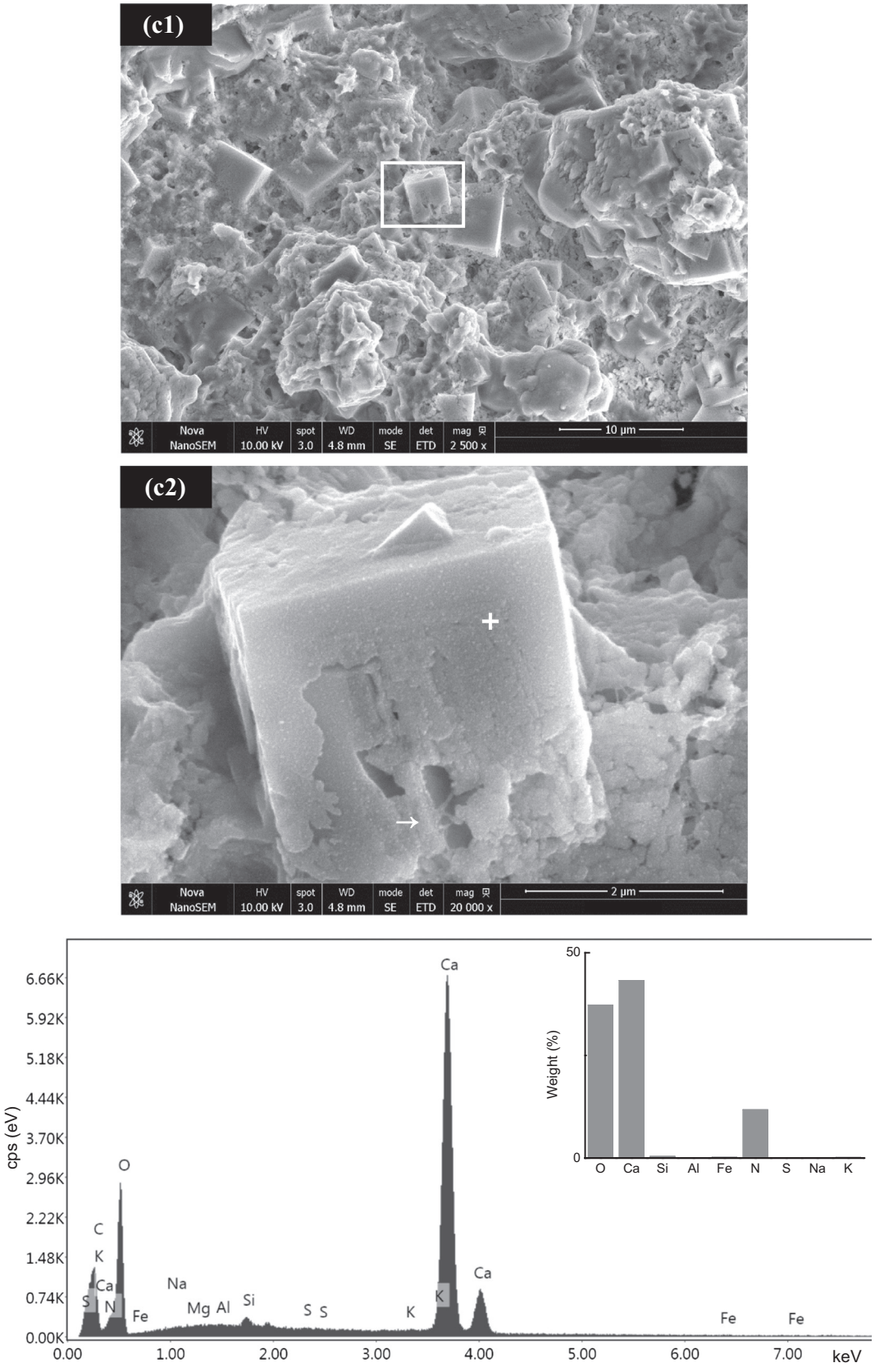

Fig. 10 (*continued*)

makes it easier to adsorb bacterial cells (Fig. 4). This adsorption created a favorable microenvironment for bacteria. It is more important that the whole particle can act as a support and protect the bacteria from squeezing in aged concrete. The LF-NMR analysis confirmed that the particles can accommodate spores as some pores with diameters of 0.6–1.6 μm were filled with spores. Thus, although a loss of ureolytic activity and a delay of cell growth occurred by encapsulation, it is still worthwhile because a potential protection can be provided by the carrier.

4.1.2. Compatibility between encapsulation material and healing agents

The influence of encapsulation material on the bacteria was first investigated. The pH of this type of cementitious material is the main aspect we concerned. Although the alkalinity of calcium sulphoaluminate cement was lower than that of Ordinary Portland cement, it was still rather high for the survival of bacteria (Fig. 1). Here, we tested the binder solution with a large w/b ratio of 10. The pH of the binder solution made from Ordinary Portland cement and calcium sulphoaluminate cement was close to 13 and around 11, respectively. Bang et al. [11] reported that an optimal pH value for the enzymatic activity of ureolytic bacteria was around 8, beyond which the activity declined gradually. Substantial amount of urease activity still remained even at pH of 10. In order to further reduce the pH of the encapsulation material, silica fume was added in varied dosages. The reduction of pH was mainly attributed to the consumption of alkali by the high pozzolanic activity of silica fume. However, an increased amount of silica fume from 20% to 40% could not reduce the pH in further, but had a negative effect on the workability of the mixture. Therefore, the formula of the encapsulation material was set as calcium sulphoaluminate cement together with 20% silica fume.

On the other hand, the influence of spores and nutrients on the encapsulation material was explored. It was first confirmed that the addition of spores with the present dosage would not have a negative effect on hydration (Fig. 2). As another part of the healing agents, organic nutrients including peptone and beef extract were essential for the germination of spores. However, direct addition of organic additives into concrete was not recommended because organic matters could result in unwanted strength loss of concrete [46]. This was reasoned by the fact that organics have a negative effect on the hydration of cementitious materials. In this paper, organics were tried to incorporate in the encapsulation material. Different dosages of organics together with spores were compared to find out the optimal content, as indicated by the setting time (Fig. 2). The addition of organics was set as 1.5% in mass of calcium sulphoaluminate cement, beyond which the setting time increased markedly. Therefore, each gram of dry encapsulated powder contained 5.5 mg peptone and 3.3 mg beef extract.

4.1.3. Compatibility between encapsulation material and concrete matrix

In prior works, many protective carriers have been studied and achieved success; however, most of the carrier materials were heterogeneous to concrete matrix [31,33,36,37,39,40]. As for calcium sulphoaluminate cement, the constituent of its hydration products was mainly ettringite (Fig. 4a), which is one of the components found in Ordinary Portland cement-based concrete. If used properly, the dilatability of ettringite can compensate the shrinkage, which is the primary cause of concrete cracking. As presented in Table 4, no appreciable variation of compressive strength was noted by the addition of encapsulation material. It indicated that the encapsulation material made by calcium sulphoaluminate cement has a good compatibility with concrete.

4.1.4. Cost and application

The cost of the microbial-based self-healing system consists of the price of the product and the treatment. The theoretical cost of the product depends on the price of the microorganism, the nutrients, and the carrier material. In China, the price of concrete amounts to about 120–200 ¥·t^{-1}. An additional cost of the bacteria, the nutrients, and the carrier material were estimated as 10 ¥·t^{-1}, 80 ¥·t^{-1}, and 50 ¥·t^{-1}, respectively, according to the mix proportions mentioned above. In addition, the cost of the treatment would be between 20 ¥·t^{-1} and 30 ¥·t^{-1}. Although the total cost was expected to be doubled, a substantial added value should be taken into account. This is largely attributable to the concept that manual inspection and repair in the whole service life of the concrete structures can be reduced. Furthermore, the fabrication procedure of the encapsulation is facile and efficient, which makes it readily applicable in practice due to a plentiful of specialist work exempted.

4.2. Autogenous healing and microbial autonomous healing

This approach was significant to prove the concept of microbial self-healing concrete by using ureolysis bacteria loaded in calcium sulphoaluminate cement-based carriers. Autogenous crack healing performance was first evidenced by the reference specimens. The maximum width of cracks can be healed was less than 100 μm, which is consistent with other researches. Major reasons of autogenous healing were generally categorized by four processes: (i) chemical precipitation of $CaCO_3$ or $Ca(OH)_2$, (ii) hydration of unhydrated cement particles, (iii) blockage due to the accumulation of impurities or broken pieces, (iv) swelling of the cement matrix [21,31]. The addition of nutrients helped to improve the crack healing performance compared with the plain mortar. Similar findings were also reported in previous researches [31,40]. The better healing performance of the abiotic control specimens than the reference ones was mainly attributed to the difference in calcium concentration and the growth of miscellaneous microorganisms. The concentration of calcium ions was a primary parameter that contributes to the precipitation of $CaCO_3$. An increase of calcium concentration, which derives from the inclusion of $Ca(NO_3)_2$ by the addition of nutrients, could promote the formation of $CaCO_3$. The miscellaneous microorganisms could come from the contamination by the air and concrete itself because the incubation operation was carried out under non-sterile conditions. Leaching of nutrients from the cracks into water would trigger the growth of co-occurring bacteria, and in turn produce metabolic $CaCO_3$ by-products. Nonetheless, the maximum width of healed cracks was limited to 250 μm for the abiotic specimens. Once pure strains were introduced, not only the width of healed cracks, but the crack healing ratio was greatly improved. This microbial autonomous healing was apparently due to the formation of $CaCO_3$ upon the ureolytic activity of bacteria. Urea from the crack walls was decomposed by bacteria and led to the production of additional carbonate ions. Thus, the $CaCO_3$ precipitation was enhanced to enable closure of larger size of cracks.

Considerable improvements by bacterially-induced autonomous healing were also manifested by the mechanical and water sorption results. The microbial specimens showed an increase of 130% and 50% in the regain ratios of compressive strength and water tightness compared to the reference ones. In contrast, increment of only 25% and 35% in the regain ratios of compressive strength and water tightness were observed for the abiotic control specimens compared to the reference ones. A much lower strength regain ratio for abiotic control specimens is due to the fact that precipitates were more likely to fill the cracks but not cement the crack walls. Close inspections on Fig. 6 show that the cracks of the abiotic control ones were filled with loose packed particles

via precipitation, compared to the tightly-sealed cracks for microbial autonomous healing. The filling might not be effective in the strength properties recovery, but it was still helpful for improving the water tightness of the specimens.

4.3. Perspectives of microbial self-healing for cracks in concrete

The microbial autonomous self-healing showed its superiority in restoring both the mechanical properties and durability of concrete by the way of encapsulating bacterial spores into low alkali cementitious materials. It is imperative to point out that the self-healing treatment conditions were still limited to experimental wet-dry cycling in this work. Realistic curing conditions in the field, particularly the water supply, should be extended to in future works. Moreover, the long-term performances of the precipitates and their bonding with the matrix are worthy of an in-depth study.

5. Conclusions

A low-alkali cementitious material made by calcium sulphoaluminate cement with 20% silica fume was developed as a useful protective carrier for ureolysis-based bacterial self-healing system in concrete. Bacterial spores were successfully encapsulated into the carrier. Although the encapsulation resulted in a loss of viability, the bacterial activity could be preserved over a long period. Besides, the compatibility of the carrier material with healing agents and concrete matrix was optimized.

The crack healing efficiency achieved by the combined use of low-alkali carrier and microbial $CaCO_3$ precipitation was evaluated by the quantitative image analysis, mechanical performance, and capillary water absorption tests. Self-healing of cracks up to 417 μm with almost complete crack closure was obtained in 28 days. The regain ratio of compressive strength and water tightness increased 130% and 50% compared with the plain mortar.

Acknowledgements

This work was supported by National Natural Science Foundation of China (No. 51378011), by Shanghai Municipal Natural Science Foundation of China (No. 17ZR1441900) and National Key Research and Development Program of China (No. 2016YFC0700802). The authors would like to thank Mrs. Wenwen Yu for technical assistance in LF-NMR tests.

References

[1] E. Boquet, A. Boronat, A. Ramos-Cormenzana, Production of calcite (calcium carbonate) crystals by soil bacteria is a common phenomenon, Nature 246 (1973) 527–529.
[2] W. De Muynck, N. De Belie, W. Verstraete, Microbial carbonate precipitation in construction materials: A review, Ecol. Eng. 36 (2) (2010) 118–136.
[3] W.R. Finnerty, M.E. Singer, Microbial enhancement of oil recovery, Nat. Biotechnol. 1 (1983) 47–54.
[4] F.A. MacLeod, H.M. Lappin-Scott, J.W. Costerton, Plugging of a model rock system by using starved bacteria, Appl. Environ. Microbiol. 54 (6) (1988) 1365–1372.
[5] U.K. Gollapudi, C.L. Knutson, S.S. Bang, M.R. Islam, A new method for controlling leaching through permeable channels, Chemosphere 30 (4) (1995) 695–705.
[6] S. Castanier, G. Le Metayer-Levrel, J.P. Perthuisot, Ca-carbonates precipitation and limestone genesis - the microbiogeologist point of view, Sediment. Geol. 126 (1–4) (1999) 9–23.
[7] P. Tiano, L. Biagiotti, G. Mastromei, Bacterial biomediated calcite precipitation for monumental stones conservation: methods of evaluation, J. Microbiol. Meth. 36 (1–2) (1999) 139–145.
[8] C. Rodriguez-Navarro, M. Rodriguez-Gallego, K.B. Chekroun, M.T. Gonzalez-Muñoz, Conservation of ornamental stone by myxococcus xanthus-induced carbonate biomineralization, Appl. Environ. Microbiol. 69 (4) (2003) 2182–2193.
[9] J.K. Mitchell, J.C. Santamarina, Biological considerations in geotechnical engineering, J. Geotech. Geoenviron. Eng. 131 (10) (2005) 1222–1233.
[10] W. De Muynck, K. Verbeken, N. De Belie, W. Verstraete, Influence of urea and calcium dosage on the effectiveness of bacterially induced carbonate precipitation on limestone, Ecol. Eng. 36 (2) (2010) 99–111.
[11] S. Stocks-Fischer, J.K. Galinat, S.S. Bang, Microbiological precipitation of $CaCO_3$, Soil. Biol. Biochem. 31 (11) (1999) 1563–1571.
[12] K.L. Bachmeier, A.E. Williams, J.R. Warmington, S.S. Bang, Urease activity in microbiologically-induced calcite precipitation, J. Biotechnol. 93 (2) (2002) 171–181.
[13] F. Hammes, W. Verstraete, Key roles of pH and calcium metabolism in microbial carbonate precipitation, Rev. Environ. Sci. Biotech. 1 (1) (2002) 3–7.
[14] S.S. Bang, J.J. Lippert, U. Yerra, S. Mulukutla, V. Ramakrishnan, Microbial calcite, a bio-based smart nanomaterial in concrete remediation, Int. J. Smart Nano Mater. 1 (1) (2010) 28–39.
[15] R. Siddique, N.K. Chahal, Effect of ureolytic bacteria on concrete properties, Constr. Build. Mater. 25 (10) (2011) 3791–3801.
[16] V. Achal, A. Mukherjee, A review of microbial precipitation for sustainable construction, Constr. Build. Mater. 93 (2015) 1224–1235.
[17] L.S. Wong, Microbial cementation of ureolytic bacteria from the genus Bacillus: a review of the bacterial application on cement-based materials for cleaner production, J. Clean. Prod. 93 (2015) 5–17.
[18] J.Y. Wang, Y.C. Ersan, N. Boon, N. De Belie, Application of microorganisms in concrete: a promising sustainable strategy to improve concrete durability, Appl. Microbiol. Biot. 100 (7) (2016) 2993–3007.
[19] M. Wu, B. Johannesson, M. Geiker, A review: Self-healing in cementitious materials and engineered cementitious composite as a self-healing material, Constr. Build. Mater. 28 (1) (2012) 571–583.
[20] H.L. Huang, G. Ye, C.X. Qian, E. Schlangen, Self-healing in cementitious materials: Materials, methods and service conditions, Mater. Des. 92 (2016) 499–511.
[21] E. Tziviloglou, K. Van Tittelboom, D. Palin, J. Wang, M.G. Sierra-Beltran, Y.C. Ersan, R. Mors, V. Wiktor, H.M. Jonkers, E. Schlangen, Bio-based self-healing concrete: from research to field application, Self-healing Mater. (2016) 345–386.
[22] S.S. Bang, J.K. Galinat, V. Ramakrishnan, Calcite precipitation induced by polyurethane-immobilized Bacillus pasteurii, Enzyme Microb. Technol. 28 (4–5) (2001) 404–409.
[23] S.K. Ramachandran, V. Ramakrishnan, S.S. Bang, Remediation of concrete using micro-organisms, ACI Mater. J. 98 (1) (2001) 3–9.
[24] J.L. Day, V. Ramakrishnan, S.S. Bang, Microbiologically induced sealant for concrete crack remediation, American Society of Civil Engineers 16th Engineering Mechanics Conference, Seattle American, 2003.
[25] J. Wang, J. Dewanckele, V. Cnudde, S. Van Vlierberghe, W. Verstraete, N. De Belie, X-ray computed tomography proof of bacterial-based self-healing in concrete, Cem. Concr. Compos. 53 (7) (2014) 289–304.
[26] H.M. Jonkers, Self Healing Concrete: A Biological Approach, Self-healing Materials, An Alternative Approach to 20 Centuries of Materials Science, Springer, 2007, pp. 195–204.
[27] H.M. Jonkers, A. Thijssen, G. Muyzer, O. Copuroglu, E. Schlangen, Application of bacteria as self-healing agent for the development of sustainable concrete, Ecol. Eng. 36 (2) (2010) 230–235.
[28] H.M. Jonkers, Bacteria-based self-healing concrete, HERON 56 (1–2) (2011) 1–12.
[29] M. Luo, C.X. Qian, R.Y. Li, Factors affecting crack repairing capacity of bacteria-based self-healing concrete, Constr. Build. Mater. 87 (2015) 1–7.
[30] M. Luo, C.X. Qian, Influences of bacteria-based self-healing agents on cementitious materials hydration kinetics and compressive strength, Constr. Build. Mater. 121 (2016) 659–663.
[31] Y.C. Ersan, E. Hernandez-Sanabria, N. Boon, N. de Belie, Enhanced crack closure performance of microbial mortar through nitrate reduction, Cem. Concr. Compos. 70 (2016) 159–170.
[32] Y.C. Ersan, H. Verbruggen, I. De Graeve, W. Verstraete, N. De Belie, N. Boon, Nitrate reducing $CaCO_3$ precipitating bacteria survive in mortar and inhibit steel corrosion, Cem. Concr. Res. 83 (2016) 19–30.
[33] V. Wiktor, H.M. Jonkers, Quantification of crack-healing in novel bacteria-based self-healing concrete, Cem. Concr. Compos. 33 (7) (2011) 763–770.
[34] R. Mors, H. Jonkers, Practical Approach for Production of Bacteria-based agent-contained Light Weight Aggregates to make Concrete Self-healing, International Conference on Self Healing Materials, Ghent, Belgium, 2013, pp. 240–242.
[35] M.G. Sierra-Beltran, H.M. Jonkers, E. Schlangen, Characterization of sustainable bio-based mortar for concrete repair, Constr. Build. Mater. 67 (Part C) (2014) 344–352.
[36] J. Wang, K. Van Tittelboom, N. De Belie, W. Verstraete, Use of silica gel or polyurethane immobilized bacteria for self-healing concrete, Constr. Build. Mater. 26 (1) (2011) 532–540.
[37] J.Y. Wang, N. De Belie, W. Verstraete, Diatomaceous earth as a protective vehicle for bacteria applied for self-healing concrete, J. Indus Microbiol. Biotech. 39 (4) (2011) 567–577.
[38] J.Y. Wang, S.V. Vlierberghe, P. Dubruel, W. Verstraete, N.D. Belie, Hydrogel encapsulated bacterial spores for self-healing concrete: Proof of concept, The 4th international conference on self-healing materials, Gent, Belgium, 2013.
[39] J.Y. Wang, D. Snoeck, S. Van Vlierberghe, W. Verstraete, N. De Belie, Application of hydrogel encapsulated carbonate precipitating bacteria for approaching a realistic self-healing in concrete, Constr. Build. Mater. 68 (6) (2014) 110–119.
[40] J.Y. Wang, H. Soens, W. Verstraete, N. De Belie, Self-healing concrete by use of microencapsulated bacterial spores, Cem. Concr. Res. 56 (5) (2014) 139–152.

[41] J. Xu, W. Yao, Multiscale mechanical quantification of self-healing concrete incorporating non-ureolytic bacteria-based healing agent, Cem. Concr. Res. 64 (1) (2014) 1–10.
[42] A.S.T.M. Standard, Standard Test Methods for Time of Setting of Hydraulic Cement by Vicat Needle, ASTM International, West Conshohocken, PA, 2004.
[43] W.P. Halperin, J.-Y. Jehng, Y.-Q. Song, Application of spin-spin relaxation to measurement of surface area and pore size distributions in a hydrating cement paste, Magn. Reson. Imaging 12 (2) (1994) 169–173.
[44] J.-Y. Jehng, Microstructure of Wet Cement Pastes: A Nuclear Magnetic Resonance Study, Engineering, MaterialsScience, Northwestern University, USA, 1995.
[45] L.A. Douglas, J.M. Bremner, Extraction and colorimetric determination of urea in soils, Soil Sci. Soc. Am. J. 34 (6) (1970) 859–862.
[46] H.M. Jonkers, E. Schlangen, Development of a Bacteria-based self Healing Concrete, Taylor & Francis Group, London, 2008.